2nd Indian International Conference on Artificial Intelligence (IICAI-05)

A Method for Automatic Segmentation of Collapsed Colons at CT Colonography

Tarik A. Chowdhury, Paul F. Whelan and Ovidiu Ghita

Vision Systems Group, Dublin City University, Ireland
{tarik, whelanp, ghitao}@eeng.dcu.ie

Abstract. This paper details the development of a novel method for automatic segmentation of collapsed colon lumen based on a prior knowledge of colon geometrical features and anatomical structure. After the removal of surrounding air voxels and lungs from the volumetric *Computed Tomography*(CT) data, labelling was performed to detect the remaining air voxel regions inside the *CT* data. Volume by length analysis, orientation, length, end points, geometrical position in the volumetric data, and gradient of centreline of each labelled air region were used as geometrical features to automatically segment the colon in CT data. The proposed method was validated using a total of 115 datasets. Collapsed colon surface detection was always higher than 95% with an average of 1.07% extra colonic surface inclusion. When the devised segmentation technique was applied to well-distended colon surface the colon detection was close to 100%.

1 Introduction

Colon cancer is the second leading cause of cancer deaths in the developed nations [1–3]. Early detection and removal of colorectal polyps via screening is the most effective way to reduce colorectal cancer (CRC) mortality [4–7]. Colonoscopy is widely considered the standard diagnostic technique for detection of colonic neoplasia [8, 9]. However, colonoscopy is an invasive, time consuming and expensive medical investigation [10]. Virtual Colonoscopy (VC) or CT colonography (CTC) [11–14] is a minimal invasive alternative medical procedure to conventional colonography. It reduces the time, cost, and patient risk when compared to traditional colonoscopy. In CTC, detection of polyps and cancerous lesions depends on the accurate identification of the colon wall and consequently relies heavily on colonic distension and bowel preparation. Currently, two types of bowel preparation are widely used in CTC. The first involves a colonic lavage and insufflation with air prior to imaging (non-oral contrast enhanced). The second involves colonic lavage and the introduction of an iodinated contrast agent to homogeneously liquefy and opacify the faecal stream prior to air insufflations (oral-contrast enhanced). Most existing automatic colonic surface detection techniques are proposed for the oral-contrast enhanced patient preparation [10, 15–17] while limited documented research is available for automatic colonic surface detection for the non-oral contrast enhanced patient preparation ([18–20]).

Bhanu Prasad (Editor): IICAI-05, pp. 3517-3532, 2005.

Masutani et al.[18] proposed a method to remove the lung tissues, surrounding air voxels, bones from the dataset and then identify the largest air volume as the colon. If a collapse appears in the colon, the largest volume was assigned as the colon and the other areas having volume 25% (Volume threshold (R_{fc})) of the largest volume were considered as parts of the colon too. As this technique evaluates the air regions only with respect to the R_{fc} threshold, parts of the small bowel can be misinterpreted as part of the colon by the automatic segmentation process. On the other hand, small parts of the collapsed colon may be incorrectly removed. Nappi et al. [19] proposed a different segmentation method that detects the colon as the intersection of Anatomy Based Extracted (ABE) surface with Colon Based Extracted (CBE) surface. ABE uses the same volumetric features proposed by Masutani et al.[18]. In CBE method, a 3D region growing was initiated from the rectum and this process continues until a stopping rule that checks for certain experimentally validated conditions is upheld. If the conditions were not met, region growing process was re-started from an automatically selected new seed point and the stopping rule is re-evaluated. Finally, the intersection surface between ABE and CBE was declared as the colon surface. This method reduced the extra-colonic surface inclusion from 25.6% to 12.6%. More recently Lordanescu et al. [20] proposed an automatic seed placement method using one seed point near the rectum for well-distended colon and two seed points at rectum and cecum for collapsed colon segmentation. Their method shows 83.2% complete colon segmentation and 9.6% partial colon segmentation. The remaining 7.2% section of the colon requires a manual seeded segmentation.

All the above discussed segmentation techniques show different levels of accuracy and indicate that further investigations are needed in order to obtain a robust technique for automatic segmentation of collapsed colons especially for non-oral contrast-enhanced patient preparation. In this paper we propose a novel method for automatic segmentation of collapsed colon lumen based on a prior knowledge of colon geometrical features and anatomical structure.

2 Automated Segmentation of Collapsed Colon

In CTC, the presence of high contrast gas/tissue interface in the air insufflated colon makes the segmentation of the colon lumen a relatively simple task. However, automatic segmentation of the entire colon has to address two major problems. Firstly, in CT data the colon is not the only gas filled organ, it also includes the gas filled lung, stomach and small bowel. In particular the small bowel may confuse the automatic colon segmentation process. Secondly, obstructions can occur in the colon itself due to peristalsis, residual faeces, water and insufficient air insufflation. Such obstructions can create multiple collapses in the colon and the complexity of the automatic colon segmentation is significantly increased. Our method initially removes the surrounding air voxel and lung tissues from the volumetric CT data while the next step identifies and labels all remaining air regions in the volumetric data. Volume by length (V/L) analysis, orientation,

length, end points, geometrical position in the volumetric data, and gradient of centreline of each labelled object were used as the geometrical features for automatic colon segmentation. Consequently, our automatic segmentation technique includes outer air segmentation, lung segmentation, labelling, V/L analysis, gradient of centreline calculations.

2.1 Surrounding Air Voxel Removal

Colon detection begins with the removal of surrounding air voxels that was performed using a standard seeded 3D region growing algorithm [24]. Seed points for 3D region growing were selected from the left-most and right-most columns voxels of first slice of the volumetric data. The threshold employed to evaluate the similarity measure for region growing was automatically selected from the global histogram as illustrated in Figure 1.

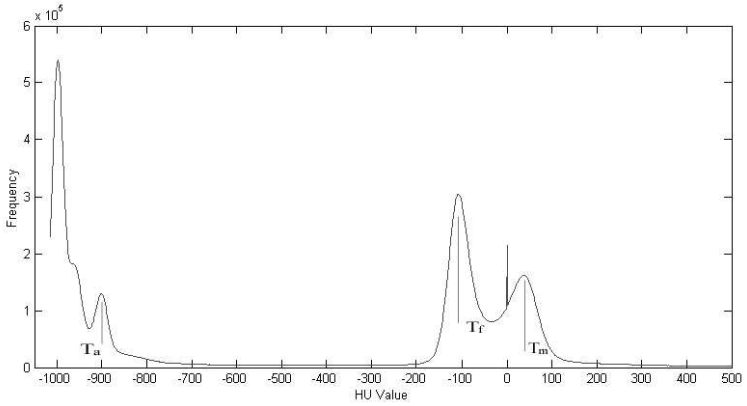

Fig. 1. Global Histogram of the CT volumetric data. T_a is the threshold used for the 3D region growing. T_f and T_m represents the histogram peaks for fat and lean tissue respectively.

2.2 Lung Detection

In all head first supine or prone volumetric CT data the lungs are always visible in the first slice. Consequently, after removal of the surrounding air voxel, 3D region growing starting in the first slice of the volumetric data will segment the lung tissues. To detect the lung, the proposed algorithm checks for the presence of isolated blood vessels inside the segmented area (see Figure 2). If multiple isolated blood vessels are detected, the segmented area is defined to be lung tissue; otherwise it is defined to be a candidate region for the colon structure.

Based on the analysis of the 25 datasets local histogram (calculated from the first five slices of the volumetric data), it was found that a threshold greater than -800HU returns the best segmentation for blood vessels from the surrounding lung air. Hence the segmentation threshold was set to -800HU.

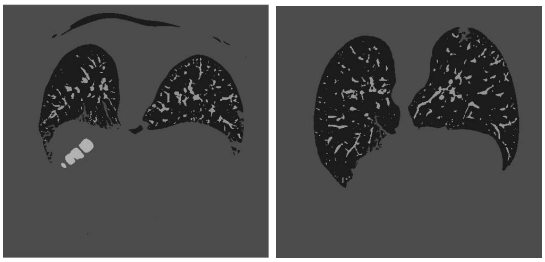

(a) (b)

Fig. 2. Detected lung from the first slice of the volumetric data. (a) Shows part of colon (in yellow) and lung. (b) Detected lung (in red). Vessels are marked in green in both (a) and (b) (Results best viewed in colour).

2.3 Labelling the Inside Area

Once the lungs have been segmented, the remaining air regions are the colon, small intestine and a few external objects (remains of SAVR). In this step, labelling was performed using a 42/46-neighbourhood 3D region growing algorithm (see Figure 3). 42 neighbourhood region growing was used if the voxel width or height was higher than 0.611mm, otherwise a 46 neighbourhood was used (in general, voxel dimensions are: depth 1.5mm, width or height 0.50-0.90mm). The 42/46 neighbourhoods are used to make the region growing approximately isotropic. The threshold for region growing was automatically selected from the global histogram and is usually in the range -800HU to -900HU. The labelling of the air regions was performed in two phases. In the first phase, any air voxels (less than the threshold) in the volumetric data initiates the region growing and continue to label all the connected air voxels. The region growing process will stop when no neighbouring voxel with *HU* values less than the threshold are found. The last voxel where the region growing stopped was considered as the *first end point* (FEP) (see Figure 4a) of that labelled region. In the second phase, region growing starts from the first end point and labels all the voxels in the region that are already checked in the first phase of labelling. At the end of the second phase, the last voxel where the region growing stopped was considered as the *second end point* (SEP) (see Figure 4b). Similarly, all the air regions in

the volumetric data will be labelled two times to calculate the two end points. During the labelling process the following information is also stored for each labelled region: total voxel count, flag value, average HU value, region bounding box coordinates and orientation.

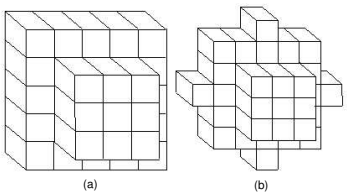

Fig. 3. Seeds used for region growing. (a) 42 voxels seed. (b) 46 voxels seed.

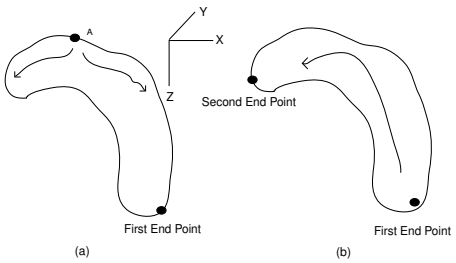

Fig. 4. Labelling using 3D region growing. (a) shows the detection of first end point and (b) shows the detection of second end point.

The *high end point* (HEP) illustrated in Figure 5a is detected as the *FEP* at the end of first phase of labelling. In the second phase, region growing starts from the *HEP* and the algorithm is iterated until the *second end point* (SEP) is detected. For this situation, the labelled region will be assigned as $ORIENT\_2$. Similarly, orientation number for each labelled region is recorded as $ORIENT\_1$, $ORIENT\_3$ or $ORIENT\_4$ as illustrated in Figures 5a, 5c, 5d. It is worth noting that for a well-distended colon supine view the orientation $ORIENT\_4$ will never occur.

2.4 Colon Detection

The colon and small intestine are approximately 1.5m and 7-10m long respectively[25]. Anatomy of the colon shows that it is shorter and thicker than the

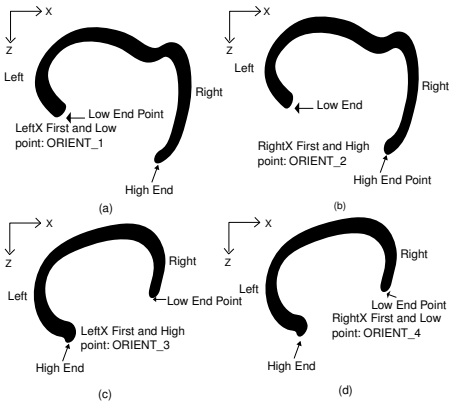

Fig. 5. The four possible orientations used to differentiate a well-distended colon and a collapsed colon.

small intestine. The volume of each labelled region is calculated using the following equation:

$$Volume = vx * vy * vz * n \tag{1}$$

where vx, vy and vz are the voxel width, height and depth respectively and n is total no of voxel in the region.

The length of each labelled region was calculated between the two end points using the Dijkstra shortest path algorithm [21]. In Figure 6 the V/L analysis for 35 datasets is illustrated. The upper and lower curves represent the colon's V/L and small intestine's V/L respectively. As the small bowel is long and thin when compared to the large bowel, V/L analysis provides a distinctive feature for automatic colon detection.

In general, the V/L value for a well-distended colon is higher than $600mm^2$. To provide a high degree of tolerance in V/L threshold, we determined experimentally that a well-distended colon must have a V/L value higher than $300mm^2$. Our results indicate that this V/L threshold was robust when the segmentation algorithm was applied to a large number of datasets.

2.5 Well Distended (Intact) Colon Detection

The devised algorithm firstly checks whether the colon has a collapsed segment or not. The algorithm is initiated with the detection of the rectum. In general, the rectum is the only air filled area that is located at the end of the dataset. To make sure that the selected object is inside the body, the voxels with HU value located around its neighbourhood are tested within a circular region of interest. The colon will be declared as intact if the selected rectum object fulfills certain conditions.

a) Detected rectum must have a V/L value higher than $300mm^2$, a length higher

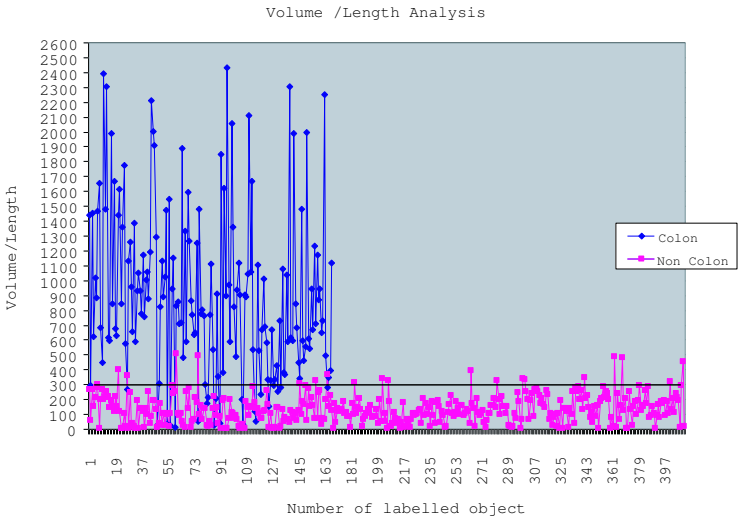

Fig. 6. Volume/Length analysis provides a distinctive feature to differentiate colon from small bowel.

than 700mm. Detected rectum length higher than 700mm means it is connected with sigmoid colon and descending colon. In this condition, if collapses appear between transverse and descending colon or transverse and ascending colon, V/L value of the rectum will be less than V/L value of the ascending colon and consequently the colon will be assumed to be collapsed.
b) Detected rectum object orientation number (Figure 5) must not be $ORIENT\_4$ for supine data and $ORIENT\_1$ for prone data.
c) Validation of the colon geometry. Projection of well-distended model for colon in the XZ plane will be similar to that depicted in Figure 7. The geometrical approximation of the colon was calculated dynamically from the labelled regions ($V/L > 100mm^2$) coordinates (left most, right most, top, bottom, front and back) as indicated in Figure 7. Sometimes collapses in the sigmoid colon can create object with a V/L value less than $300mm^2$ and to include all these objects we fixed the threshold to $100mm^2$. For a well-distended colon, the air region detected as rectum will have one end point (rectum point) near the rectum and other end point (cecum point) closer to the cecum. To declare the detected labelled air region as well-distended colon, part of it must fulfills the ascending and descending colon geometry (see Figure 7). Otherwise it will be declared as collapsed colon.

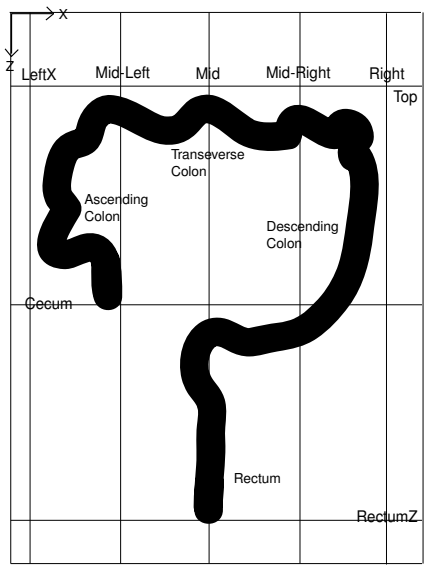

Fig. 7. An ideal model for a well-distended colon structure.

2.6 Collapsed Colon Detection

Collapsed colon detection is performed in two phases. In the first phase, large segments (with $V/L > 300$) are detected and in the second phase small objects (with $V/L < 300$) are detected. The detection of large segments starts from the rectum. It detects the closest placed large segments using the Euclidean distance between the end points (Figure 8) and checks for the condition (a) and (c) which are detailed in the Section 2.5. This process continues until the condition (a) and (c) are met. It is worth noting that in some cases detection of the ascending colon appears after the rectum (clockwise detection) as depicted in Figure 8b. This condition occurs if large parts of the descending colon and sigmoid colon are filled with residual material. In this situation the V/L threshold is automatically changed to $200mm^2$ to meet the geometrical condition (c) described in Section 2.4. Small-labelled areas (with $V/L < 300$) are either part of the small intestine or the colon. As their anatomical and geometrical properties are quite similar, perfect colon identification is far from a trivial task. Our segmentation scheme analyses the small segments (with $V/L < 300$) using their position, gradient of the centreline, length, and distance.

Centreline and gradient detection: Initially centrelines of each labelled air region were detected using the method described by Sadleir and Whelan [22]. To reduce the noise in the centreline detection, we employed a three-step procedure [23]. Firstly, a second order low pass filter was applied to remove the high frequency components of the centreline. Secondly, the filtered centreline was down-sampled (typically by a factor of seven). Thirdly, three cubic B-spline interpolations were

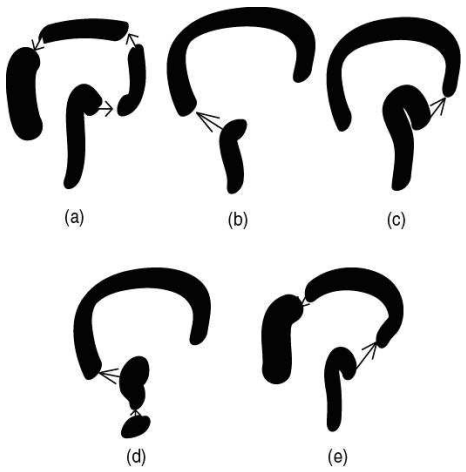

Fig. 8. Examples of $V/L > 300$ object detection in collapsed colon for supine data. a) Four $V/L > 300$ in expected direction. b) Two $V/L > 300$ in anti clockwise direction. c) Two $V/L > 300$ in expected direction. d) Anti clockwise direction occurred in the third object. e) Object detected in expected direction.

constructed for the resulting down-sampled set of points (one for each of the three orthogonal directions). The gradient of the centreline was calculated using the first derivative of the interpolated centreline. *Grad/Num* was calculated using the following equation:

$$Grad/Num = 1/n \sum grad \tag{2}$$

where *grad* is the gradient in each voxel and n is the number of voxel in the centreline.

Figures 9a to 9c show three colon large segments (with $V/L > 300$) and few small segments (with $V/L < 300$) which are either part of the colon or small bowel. In first step, small objects placed between the large segments 1 and 2 depicted in Figure 9 will be detected, and in the second step small objects between the large segments 2 and 3 will be detected. Small objects *ii*, *iii* and *iv* shown in Figure 9a have one end point near to the large segment *1* and other end point near to the large segment *2* or *3*. So, their locations violate the required condition and will be rejected. Similarly, all the small segments in Figure 9a will be initially rejected due to an improper location. Both small segments illustrated in Figure 9b have proper location, but they will be rejected because do not pass the length threshold test. Similarly, small segments in Figure 9c will be rejected because they do not pass the distance threshold test. The length and distance thresholds were set as twice the end points distance of large segments. For instance if the large segments 1 and 2 shown in Figure 9 have a distance between the endpoints equal to 50mm, the length and distance threshold will be

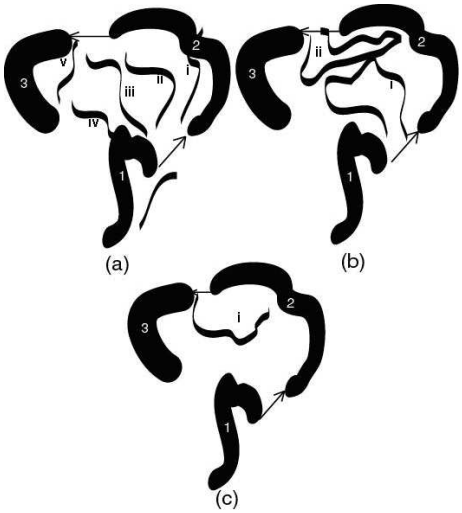

Fig. 9. Example of removing small intestine. a) Rejected six small intestine parts because of improper orientation. b) Two small intestine sections are rejected due to the length threshold. c) Rejected due to the distance threshold.

set to 100mm. As the geometry of the small bowel shows high degree of curvature when compared to the curvature of the colon, the *Grad/Num* of small bowel has a higher value then the *Grad/Num* value of the small colon parts. If the detected small segment has *Grad/Num* higher than a threshold is rejected and declared as part of the small bowel.

3 Results

The segmentation was performed on 115 supine and prone patient datasets. All patients were scanned at 120kVp, 100mAs, 2.5mm collimation, 3mm slice thickness, 1.5mm reconstruction interval, and 0.5s gantry rotation. The scanning times range from 20 to 30s, hence, acquisitions were performed in a single breath-hold. The procedure was first performed with the patient head first supine position and then repeated with the patient head first prone position. The number of slices varies from 200-350 depending on the height of the patient.
Our automatic segmentation method reliably detected 52 well-distended colons without inclusion of any Extra Colonic Surface (ECS) areas. Consequently colon surface detection was 100% and the *ECS* error was 0%. Detection of the collapsed colon was performed in several phases. Detection of large segments (with $V/L > 300$) was performed in the first phase and 142 air regions were detected in 55 datasets. Out of these 142 regions, 141 were colon parts and one was a section of the small bowel. The detection of small regions ($V/L < 300$) was done in the second phase. In total 229 ($V/L < 300$) small air regions were detected

in 55 datasets of which 101 were colon surfaces and 128 were *ECSs* and 6 colon objects were missed. In 55 collapsed colons, surface detection was always higher than 95% (see Figure 10). Only in two cases it was less than 98% (95.51 and 97.71% respectively) and in one case it was 98.15%. For the remainder of the cases it was higher than 99% out of 55 collapsed colons. Largest *ECS* detection was 11.28% with a mean of 1.07%.

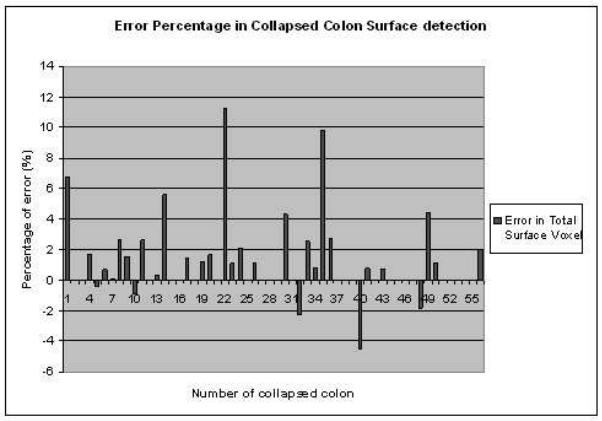

Fig. 10. Percentage of error for *ECS* and colonic surface missing in 55 collapsed colon.

To examine our automatic segmented colon surface, a human operator performed a manually seeded segmentation and we used it as the ground truth data. Initially, the operator segmented the colon manually using seed points and 3D region growing. This manual segmentation was performed in conjunction with a 3D visualization software tool. If the manually detected 3D colon view looks satisfactory the operator compared automatic segmented colon with the manually detected colon side by side. The operator also compared the automatic segmented colon with the manually segmented colon using 2D axial view. Any area which was seen in the automatic segmented colon but not found in manually segmented colon was declared as *ECS*. Thus 128 ($V/L < 300$) objects were declared as *ECS's* out of 229 ($V/L < 300$) objects.

The method proposed by Nappi et al. [19] shows an average of 12.5% *ECS* inclusion with a mean of 0.9% colonic surface missing which are higher than our average *ECS* (1.07%) inclusion and mean colonic surface missing (0.18%). Lordanescu et al. [20] method shows 83.2% success rate for complete automatic segmentation of colon. On the other hand our method provides 93.04% success rate for automatic segmentation of collapsed colon in 115 datasets.

The proposed algorithm fails to produce meaningful results when applied to 8 out of 115 datasets because of inappropriate bowel distension and insufficient colon insufflations (more than 50% of the colon area was filled with fluid and/or resid-

ual materials). Another advantage of our technique is its low computational cost where the typical processing time for overall segmentation was approximately 3min on a Pentium IV 2.2GHz PC with 512MB RAM.

4 Discussion and Conclusion

Our results indicate that our segmentation algorithm returns reliable segmentation under all routinely encountered imaging conditions. Well-distended colons have been detected without any inclusion of the small bowel (Figure 11). When dealing with collapsed colons, detection of surfaces with a $V/L > 300$ have generated only one false positive in all the datasets (Figures 12,13,14). Small cross-section areas (with $V/L < 300$) include the colon and the small intestines and show an average of 1.04% *ECS* surface inclusion and an average of 0.1802% colon surface missing. Results show that our method reliably detects well-distended colon and large segments in collapsed datasets and shows a low *ECS* inclusion in small segments detection.

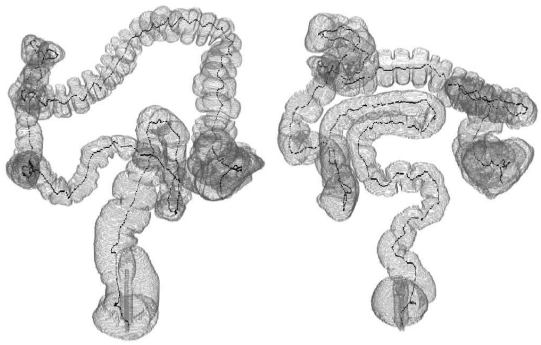

(a) (b)

Fig. 11. Iso-surface of well-distended colon with the centreline superimposed.

In this paper, a new scheme for automatic segmentation of collapsed colon is detailed based on the inclusion of geometrical feature such as V/L analysis, orientation, end points, gradient of centreline, and directions (clockwise or anticlockwise). The experimental data indicates that the V/L analysis provides a better approximation of colon to differentiate it from the small bowel. In calculation of V/L, we used morphological labelling for finding the end points and volume and shortest path algorithm for finding the length. For well-distended colon detection, the features we included in the segmentation process are V/L,

(a) (b)

Fig. 12. Collapsed colon. (a) Three colon surfaces with $V/L > 300$ and seven colon surfaces with $(V/L < 300)$ and six *ESCs* with $(V/L < 300)$. (b) Three colon surfaces with $V/L > 300$, twelve colon surfaces with $(V/L < 300)$ and eleven *ECSs* with $(V/L < 300)$.

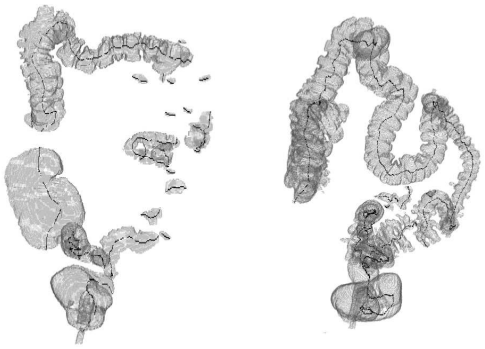

(a) (b)

Fig. 13. Collapsed colon. (a) Five colon surfaces of $V/L > 300$, nine colon parts with $(V/L < 300)$, and seven *ESCs* with $(V/L < 300)$. (b) Two colon surfaces with $V/L > 300$, one colon surface with $(V/L < 300)$ and four *ESCs* with $(V/L < 300)$.

length, orientation, and geometrical position in the volumetric data. In detection of collapsed colon large segments (with $V/L > 300$), we used the geometrical position in the volumetric data, V/L, length and direction as features. The features we used for collapsed colon small segments $(V/L < 300)$ detection are

end points, length, distance and gradient of centreline. All threshold parameters used in the automatic segmentation scheme were selected with a high degree of tolerance and they proved to be robust in the segmentation process. Any dataset without a labelled region of length less than 400mm was declared to be a poorly distended dataset and the algorithm rejects the dataset as unsuitable for automated analysis. This condition arises when the datasets have nearly 50% regions filled with residual material and fluid due to insufficient insufflation.

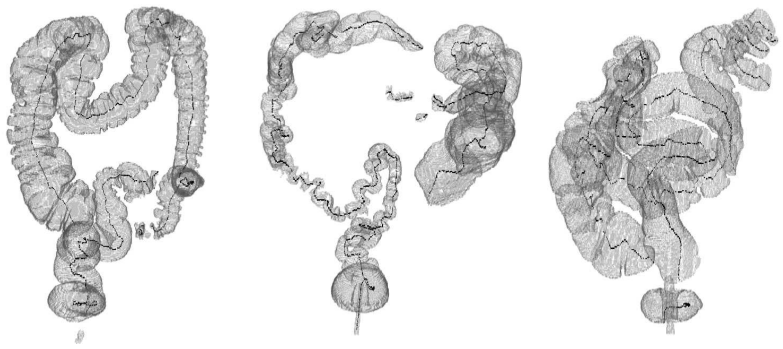

(a) (b) (c)

Fig. 14. Collapsed colon. (a) Two colon surfaces with $V/L > 300$, one colon part with $(V/L < 300)$, and one extra-colonic surface with $(V/L < 300)$. (b) Two colon surfaces with $V/L > 300$, two colon parts of $(V/L < 300)$, and two *ESCs* with $(V/L < 300)$. (c) Six colon surfaces with $V/L > 300$.

Our method successfully performs automatic segmentation of collapsed colonic lumen from volumetric CT data. In 55 supine and prone datasets containing collapsed colon data, the segmentation method successfully detects 95% of the imaged colonic walls. In 52 datasets the well-distended colons were detected without any inclusion of extra-colonic surface. The performance of our algorithm makes it suitable for 3D visualization of the colon surface and advanced polyp detection.

5 Acknowledgment

The authors would like to thank our medical collaborators Dr. Helen Fenlon, Dr. Alan O'Hare (Department of Radiology) and Dr. Padraic MacMathuna (Gastrointestinal Unit) at the Mater Misericordiae Hospital, Dublin. We would also like to acknowledge the valuable input from our colleagues from the Vision Sys-

tems Group, namely, Robert Sadleir and Nicolas Sezille. This work is funded by Science Foundation Ireland.

References

1. Parker, S., Tong, T., Bolden, S., Wingo, P.: Cancer statistics 1997. CA Cancer Journal for Clinicians (1997), 47, 5-27
2. NCRI, 2000: Cancer in Ireland, (1997): Incidence and Mortality, Healy & Associates
3. Cancer Research UK.: Bowel Cancer Factsheet April (2003).
4. Ransohoff, D. F., Sandler, R. S.: Screening for Colorectal Cancer. N Eng J Med, Vol. 346, No. 1 January 3, (2002)
5. American Cancer Society: Cancer Facts and Figures, American Cancer Society, (1999)
6. National Cancer Institute: Working guidelines for early cancer detection: Rationale and supporting evidence to decrease mortality. Bethesda: National Cancer Institute, (1987)
7. Robert, A., Cokkinides, S. V., Eyre, H. J.: American Cancer Society Guidelines for the Early Detection of Cancer, 2003. CA Cancer J Clin (2003), 53, 27-43
8. Schrock, T.R.: Colonoscopy versus barium enema in the diagnosis of colorectal cancer and polyps. Gastrointest Endosc. Clin. North. Am. (1993), 3, 585-610
9. Winawer, J.S., Stewart, E.T., Zauber, A.G., Bond, J.H.: A Comparison Of Colonoscopy and Double-Contrast Barium Enema For Surveillance After Polypectomy. The N. England Journal of Medicine, 342, 1766-1772 (2000)
10. Sato, et al.: An Automatic colon segmentation for 3D virtual colonoscopy. IEICE Trans. Information and Systems, Vol. E84-D, No. 1, pp. 201-208, January, (2000)
11. Vining. D.J., Gelfand, D.W., Bechtold R.E., et al.: Technical feasibility of colon imaging with helical CT and virtual reality [Abstract]. AJR (1994), 162:104
12. Johnson, C.D., Hara, A.K., Reed, J.E.: Virtual endoscopy: what's in a name?. AJR (1998),171:1201-2
13. Lichan, H., Arie, K., Yi Chih W., Ajay V., Mark W., Zhengrong L.: 3D Virtual Colonoscopy. In Proc. Biomedical Visualization, M. Loew and N. Gershon, Eds., Atlanta, 26-33 (1995)
14. Hara, A., et. al. Detection of Colorectal Polyps by CT Colonography: Feasibility of a novel technique. Gastroenterology, vol. 100, 284-290, (1996)
15. Wyatt, C.L., Ge, Y., Vining, D.J.: Automatic segmentation of the colon for virtual colonoscopy. Comput. Med. Imaging. Graph. (2000), 24:1-9
16. Liang, Z., et al.: Inclusion of A Priori Information in Segmentation of Colon Lumen for 3D Virtual Colonoscopy. Conf. IEEE NSS-MIC (1997), 1423-1427
17. Dongqing, C., Wax, M.R., LI L., Liang Z., LI B., Kaufman A.E.: A Novel Approach to Extract Colon Lumen from CT Images for Virtual Colonoscopy. IEEE Transactions on Medical Imaging, Vol. 19, 12, 1220-6, (2000).
18. Masutani, Y., et al.: Automated Segmentation of Colonic Walls for Computerized Detection of Polyps in CT Colonography. Journal of Computer Assisted Tomography, (2001), 25(4), 629-638
19. Napii J., Dachman, A.H., Maceneaney, P., Yoshida, H.: "Automated Knowledge-Guided Segmentation of Colonic Walls for Computerized Detection of Polyps in CT Colonography". Journal of Computer Assisted Tomography, 26(4), 493-504, July/August (2002)

20. Lordanescu, G., Pickhardt, J.P., Choi, J.R., Summers, R.M.: "Automated Seed Placement for Colon Segmentation in Computed Tomography Colonography". Acad. Radiol., (2005) 12, 182-190
21. Dijkstra, E.W.: A note on two problems in connexion with graphs. Numer Math (1959), 1:269-71
22. Sadleir, R.J.T., and Whelan P.F.: Colon Centerline Calculation for CT Colonography using Optimised 3D Topological Thinning. First international symposium on 3D data processing visualisation and transmission, (2002)
23. Sezile, N., Sadlier, R.J.T. , and Whelan, P.F.: Fast Extraction of Planes Normal to the Centerline from CT Colonography datasets. International Conference on Visual Information Engineering, (2003), 161-164
24. Gonzalez, R.C., Woods, R.E.: Digital image processing, Reading MA: Addison-Wesley, (1993)
25. Atlas of Human Anatomy, Eagle Editions, ISBN: 1-902328-40-X